

---

# REDUCING THE COST OF DROPOUT IN FLASH-ATTENTION BY HIDING RNG WITH GEMM

---

Haiyue Ma<sup>1,2</sup> Jian Liu<sup>2</sup> Ronny Krashinsky<sup>2</sup>

## ABSTRACT

Dropout, a network operator, when enabled is likely to dramatically impact the performance of Flash-Attention, which in turn increases the end-to-end training time of Large-Language-Models (LLMs). The main contributor to such performance degradation is the Random Number Generation (RNG) phase that is traditionally fused into the Flash-Attention kernel. As RNG and Attention have the same hardware bottlenecks, RNG latency can hardly be hidden within the Attention kernel.

We propose overlapping RNG with previous GEMM layers in the network to hide RNG runtime and improve end-to-end performance. RNG and GEMM have distinct resource requirements and hardware bottlenecks, so they can run in parallel without compromising each other’s performance. Our fine-grained performance model, cross-validated by silicon results, shows 1.14x speedup on one transformer block (including multi-head attention and feed-forward layers) for Llama2, and up to 1.23x speedup when varying workload sizes, on GH100 GPUs with FP8 precision. Further, we extend our theoretical model to different RNG implementations and hardware architectures, and discuss the widely applicable benefits for overlapping RNG with GEMM layers.

## 1 INTRODUCTION

Large Language Models (LLMs) have become important targets for performance optimization due to their ever-increasing workload sizes and corresponding runtime demands. Full-scaled training for models like GPT (OpenAI, 2023) requires several months and thousands of GPUs (II, 2023). Attention dropout (Srivastava et al., 2014)(Zehui et al., 2019) is an optional technique that drops out elements after the Softmax operation in Attention. Dropout is applied in commonly used models such as Llama (Face)(Touvron et al., 2023) because it can make the model focus on relevant features and improve training accuracy (Schumacher)(Shastri) (Xue et al., 2024). However, enabling dropout is costly, which doubles the processing time of the Attention layer with state-of-the-art implementations like Flash-Attention (Dao et al., 2022)(Dao, 2023)(Shah et al., 2024), and in turn increases the end-to-end training time by 1.3x to 1.7x, depending on the network parameters. Optimizing the runtime of dropout can significantly improve the performance of LLM training.

The runtime of dropout is dominated by the Random Number Generator (RNG) (Salmon et al., 2011), which generates random numbers to determine which elements within the

intermediate matrix of the Attention layer to drop. The size of this matrix, and consequently the runtime of RNG, scales quadratically with the sequence length. As the industry trends towards ever larger sequence lengths, this exacerbates the RNG latency.

Traditionally, dropout (including RNG) is fused into the Flash-Attention kernel. The Attention layer is not limited by matrix-matrix multiplication (MMA) math but rather by non-compute bottlenecks, including the Register File read and write bandwidth, the Issue Stage, and Multi-Function Operations. Because RNG is also bottlenecked by these limiters, its latency is almost fully exposed when fused with Attention. Silicon measurements shows that only 10-20% of RNG runtime can be hidden with the Attention kernel for GPT-like workload sizes.

In this paper, we propose a method to overlap RNG with other matrix multiplication (GEMM) layers within the Transformer Block to hide RNG runtime and improve end-to-end performance. The stand-alone RNG kernel generates one bit for each element to decide whether it is dropped, and write them to the memory to be read and used later by the Attention kernel when performing the dropping.

RNG and GEMM are ideal targets for overlapping because they do not depend on each other and have distinct resource requirements and hardware bottlenecks. GEMM is predominantly bounded by MMA math and L2 bandwidth, whereas RNG is mostly limited by the Issue Stage and ALU

<sup>1</sup>Princeton University, Princeton, New Jersey, USA <sup>2</sup>NVIDIA Corporation, Santa Clara, California, USA. Correspondence to: Haiyue Ma <hm1@princeton.edu>.

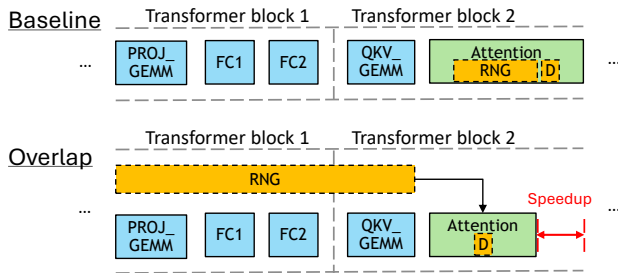


Figure 1. Dropout, including RNG, is traditionally fused in Flash-Attention. Overlapping RNG with GEMM layers before Attention hides exposed RNG latency and results in speedup.

operations. Despite GEMM consuming nearly all the Register Files (RF) and Shared Memory (SMEM) within each Streaming Multiprocessor (SM), RNG uses minimal RF and SMEM, allowing GEMM to run in parallel with RNG while obtaining near-optimal performance.

We built a fine-grained theoretical performance model for RNG and GEMM overlapping. This model analyzes hardware bottlenecks for individual kernels, fused kernels, and interference between overlapping kernels. It takes in GPU hardware configurations and the model parameters, and outputs the theoretical runtime for each kernel.

Our model is validated by silicon results running with FP8 precision (NVIDIA, e) on H100 HBM3 80GB GPUs (NVIDIA, f), showing only a 2% difference between theoretical and actual results. Results demonstrate great potential when overlapping RNG with the GEMM layers between the previous and the current Attention layer: 1.14x speedup for Llama2 (Touvron et al., 2023), 1.13x for MoE (a trillion-parameter NVIDIA model prototype (NVIDIA, h)), and 1.06x for GPT3 (Brown, 2020). We also observed up to 1.23x speedup under varying network parameters within the range of common workloads.

We extend our analysis to different hardware designs to evaluate how changes in the chip’s computing power could impact results. We also explore the adaptability of the overlapping technique with different implementations of the RNG function. Furthermore, our overlapping methodology can be generalized to other layers in the network that meet three key criteria: no data dependencies (or resolvable through pipelining), no shared hardware bottlenecks, and no capacity conflicts. Possible targets for overlapping include the Communication layer, either with GEMM or even RNG, as well as the Matrix Transpose and Precision Conversion layers if required by the network.

In this paper, we make the following contributions:

- We proposed overlapping the key component of

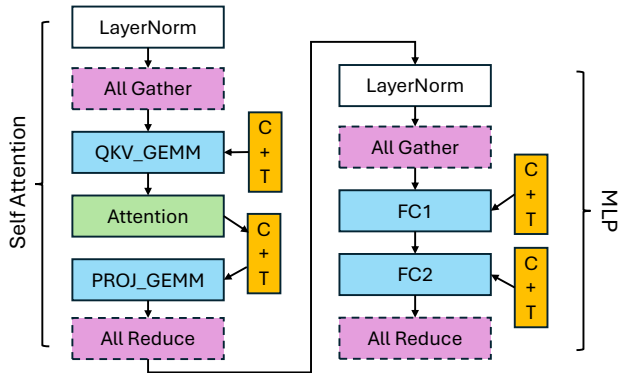


Figure 2. Network Architecture of one Transformer Block, the basic building block of LLM network. The four GEMM layers and the Attention layer dominate the runtime.

dropout, RNG, with GEMM kernels to hide RNG latency, leading to substantial speedup across multiple trending LLM architectures.

- We developed a detailed theoretical performance model for assessing the benefits of overlapping RNG and GEMM, given the workload sizes of the network and the hardware specification. The accuracy of our model is cross-validated by results obtained from real silicon implementations.
- We explored the broader implications of the overlapping mechanism for different RNG implementations, application on other targeting layers, and future hardware architecture designs.

## 2 BACKGROUND

### 2.1 LLM Network Architecture

LLM networks typically begin with an embedding layer, conclude with a decoding layer, and iteratively call Transformer Blocks in between. Figure 2 shows the network architecture of one Transformer Block in the forward path. The General Matrix Multiply (GEMM) layers in blue and the Attention layer in green contribute to the majority of the compute time. The purple dashed layers represent communication layers, present only in multi-GPU systems. The white LayerNorm layers perform element-wise operations, and the orange C+T layers handle Conversion (when precision conversion to FP8 is necessary) and Transpose operations for GEMM inputs. These last two types of layers typically require minimal runtime and are omitted from our runtime analysis.

In this work, we begin our analysis on single GPU without communication, and focus on the GEMM and Attention layers. We discuss multi-GPU scenarios in Section 5 and draw similar conclusions as in single GPU. With multi-GPU, dif-

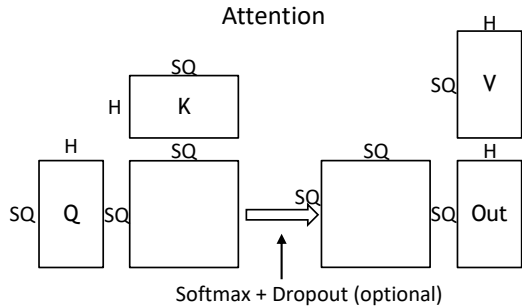


Figure 3. Dropout is applied to the intermediate results in Flash-Attention, after the Softmax operation.

ferent parallelism mechanisms (NVIDIA, g) (Shoeybi et al., 2019) are applied which evenly distribute workload onto different GPUs. This does not impact savings of overlapping since the ratio of each kernel’s runtime remains the same. In highly optimized implementations, communication layers are often overlapped with their producer layers to minimize latency overhead, therefore the end-to-end savings brought by overlapping still apply.

## 2.2 Dropout

Dropout (Srivastava et al., 2014)(Wan et al., 2013) is a technique designed to prevent overfitting by randomly setting a small fraction of the elements within a network to zero. It has been proposed to regularize neuron networks in general. In the context of this paper, we refer specifically to Attention dropout (Schumacher)(Shastri), where the dropout operation is applied to the intermediate outputs of the Attention layer following the Softmax operation, as depicted in Figure 3.

While optional, dropout can substantially improve training accuracy: it prevents the model from relying heavily on certain features, thus making the model only focus on relevant features to prevent overfitting and underfitting (Xue et al., 2024)(Liu et al., 2023). Dropout is used in training widely adapted LLM networks such as Llama2 (Face)(Touvron et al., 2023). However, its huge runtime slowdown has limited its application. We explore dropout optimizations to improve its practicality in future applications, facilitating broader implementation.

## 2.3 RNG Implementation: Philox

The computational demand of dropout mostly comes from the Random Number Generator (RNG) used to determine which elements to zero out. Multiple possible RNG implementations exist, and our discussion centers on Philox (Salmon et al., 2011) (NumPy). Philox is a counter-based pseudorandom number generator (PRNG) that relies

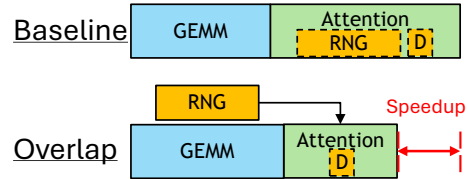


Figure 4. Setup for baseline: dropout (including RNG) fused in Attention, and overlap: stand-alone RNG running in parallel with GEMM, with output consumed by Attention. D stands for the element dropping step.

on wide multiplies and iterates over previous states to generate new ones. Philox is well-suited for GPU execution, as its operations can be efficiently parallelized. Implementations of Philox are available in NVIDIA’s cuRAND library (NVIDIA, d) and TensorFlow (TensorFlow). Our analysis primarily focuses on a seven-iteration implementation (Philox 7), though we also consider more resource-efficient versions (Philox 5 and 3) in Section 5.

## 3 IMPLEMENTATION

In this section, we discuss our experiments performed on silicon, as well as the fine-grained performance model which is backed up by silicon results. We first validate our performance assumptions that are essential for effective overlapping on silicon, then utilize the theoretical model to generalize our findings. Figure 4 shows the setup for baseline and overlap experiments.

### 3.1 Silicon Implementation

We tested a CUDA implementation of our proposal on NVIDIA H100 GPUs (NVIDIA, f), the cutting-edge option for data-center training tasks, specifically using the GH100 HBM3 80GB variant. This GPU supports the latest High Bandwidth Memory (HBM) and provides ample compute resources and memory capacity for LLM training.

For GEMM kernel analysis, we implemented QKV\_GEMM, the GEMM layer that immediately precedes the Attention layer. Since GEMM layers have predictable runtime given the M, N and K dimensions, analyzing a single GEMM layer provides sufficient data to predict behavior across all four potential GEMM layers to overlap within a Transformer Block.

In terms of implementation, RNG and GEMM can either run as separate kernels or within the same kernel using warp specialization (Li et al., 2023)(NVIDIA, i)(Kerr et al.). We opted for separate kernels to maintain a clear distinction between independent components in the network such as RNG and GEMM in this case. This approach allows other overlapping strategies to be implemented without deep knowl-

edge of the kernels’ internal complexities, especially for the highly optimized GEMM kernels. Warp specialization enables a more fine-grained overlapping and we anticipate it to bring further, but limited, performance benefits.

Our silicon implementation uses production-ready, highly optimized GEMM, Attention, and dropout kernels. GEMM tile size is consistently set at 128x128x128, while RNG and Attention use a tile size of 64x128x128. The dropout kernel was modified to run in two scenarios: 1) fused within the Attention kernel, and 2) as a stand-alone RNG kernel storing bits representing random numbers in HBM for later use by the Attention kernel. We used the Philox 7 algorithm for RNG.

### 3.1.1 Performance Assumptions

To validate our assumptions about performance impacts, we conducted several tests:

- **GEMM Resource Allocation:** Originally, the GEMM kernel utilizes all available Register Files and Shared Memory in each SM. We carved out 6% of the Registers and 7% of the Shared Memory for the RNG kernel, hypothesizing this would not adversely affect GEMM performance. Our silicon measurements confirmed only 0.5% average performance difference across various GEMM workload sizes.
- **Processing Time for Dropping Elements:** We hypothesized that dropping the elements within the Attention layer would require minimal runtime compared to RNG. Our silicon results confirmed that RNG dominated the full dropout, while dropping the elements only increase the original Attention runtime by 12% on average.
- **RNG and GEMM Interference:** We hypothesized that RNG should not noticeably slow down GEMM performance. We observed an average of 4% slowdown in GEMM when running concurrently with RNG, which is acceptable. Conversely, RNG experiences a 50% slowdown when run alongside GEMM, but this is also deemed acceptable since the original runtime of RNG is likely shorter than GEMM.

### 3.1.2 Baseline and Overlap CUDA Implementation

The baseline implementation includes a stand-alone QKV\_GEMM kernel and dropout (including RNG) fused into the Attention kernel, running serially on the same CUDA stream. Our optimized kernel fusion minimizes synchronization overhead and maximizes the overlap of RNG operations with Attention’s floating-point computations.

The overlapping implementation uses two separate CUDA streams to allow GEMM and RNG kernels to run concur-

Table 1. Hardware Limiters.

Limiters	Note
MMA Math (TFLOPS)	Max compute intensity of Matmul, main limiter of GEMM.
L2 Bandwidth	Read and write bandwidth between L2 and the SM cores.
HBM Bandwidth	Read and write bandwidth to the main memory.
RF Bandwidth	Read and write bandwidth for the Register Files within each SM.
Instruction Issue	Pipeline for issuing instructions.
ALU Pipe	Pipeline for executing ALU instructions.
Multi-Function Units Pipe	Pipeline for executing multi-function instructions.
FMA Pipe	Pipeline for executing FMA instructions.

rently. The Attention kernel is launched on the GEMM stream once both kernels have completed. This implementation minimizes the load latency of RNG states in Attention by overlapping the loads with the  $Q * K$  matrix multiplication.

Both baseline and overlapping implementations use CUD-Agraph (NVIDIA, c) to minimize delays between kernel launches and optimize overall efficiency. The GPU is warmed up using multiple instances of the captured CUDA graphs before actual measurements are taken. We validated our CUDA implementation against CPU-generated result, ensuring correctness across various batch sizes, sequence lengths, and number of heads.

## 3.2 Theoretical Model

This subsection explains the construction of our fine-grained theoretical performance model, designed to evaluate the overlapping technique’s effectiveness based on hardware bottlenecks. We begin by discussing the hardware bottlenecks taken into account in our model, and then the derivation of baseline and overlapping runtime.

### 3.2.1 Hardware Limiters

We identified several hardware limiters critical for calculating kernel runtime in our performance model. For each kernel, we estimate its runtime assuming each limiter as a potential bottleneck and determine the final runtime by selecting the maximum runtime among all considered limiters.

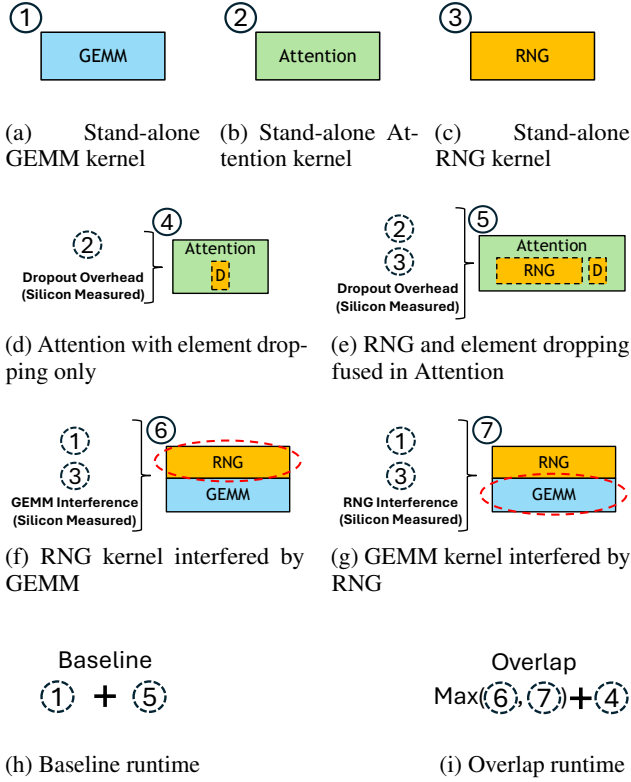


Figure 5. Theoretical performance model: modeling baseline and overlap runtime from individual kernel runtime.

### 3.2.2 Modeled Layers

Figure 5 illustrates the modeling approach for baseline and overlap runtime, incrementally constructed with individual kernel performance assessments.

Initially, we model the performance of each individual kernel - GEMM, Attention, and RNG — calculating their theoretical runtime based on bounding each by the limiters. For workload sizes within the range of typical networks (GPT (Brown, 2020) and Llama (Touvron et al., 2023)), we found that GEMM runtime is bounded by MMA, Attention by RF bandwidth and the Issue stage, and RNG by the Issue stage and ALU pipe.

Next, we integrate additional components to derive runtime estimations for composed kernels. For the Attention kernel with the element dropping step, we derive its runtime by adding the silicon-measured dropping overhead to the standalone Attention kernel runtime (Figure 5d). We also compute the runtime of the fused Attention kernel with RNG by integrating both sets of instructions and identifying the primary limiter, which typically is the Issue Stage, with the ALU pipe and RF bandwidth as close secondary limiters (Figure 5e).

We then calculate the runtime of RNG and GEMM separately while the other is running concurrently. RNG runtime is based on the stand-alone RNG, scaled by the GEMM interference overhead measured in silicon. If RNG’s runtime exceeds GEMM’s, the remaining RNG operations continue at full speed once GEMM completes (Figure 5f). Similarly, we model the GEMM runtime affected by RNG interference (Figure 5g).

Finally, we determine the baseline runtime from the standalone GEMM and the fused Attention-and-RNG kernel runtime (Figure 5h). The overlap runtime is derived from the maximum runtime of GEMM and RNG with interference, as Attention depends on both GEMM and RNG outputs, plus the standalone Attention runtime with only the element dropping step (Figure 5i).

## 4 RESULTS

This section presents the performance outcomes of our RNG and GEMM overlapping experiments. The analysis is based on the theoretical results, supported by silicon measurements. We base our experiments on a GPT-3-like network architecture, using a common hidden dimension per head of 128, and a batch size of 1. We vary the sequence lengths from 2048 to 65536, and number of heads from 48 to 128. These conclusions are broadly applicable across various network architectures.

We validated the theoretical model’s accuracy with a mere 2% average difference between the theoretical model and silicon measurements for overlapping QKV\_GEMM with RNG. The difference is calculated by averaging the absolute difference of speedup between silicon and theoretical results. With such validation, we extend our performance analysis to overlapping RNG with all four GEMM layers between the previous and the current Attention layer. Figure 6 shows the modeled overlap speedup for different sequence length and number of heads.

The results demonstrate significant performance improvements, with speedups up to 1.23x across the five key layers of a Transformer Block (four GEMM and one Attention layer). Specific speedups include 1.06x for GPT-3, 1.14x for LLAMA2, and 1.13x for MoE. Further analysis reveals that speedup is closely correlated with the ratio of sequence length to the number of heads, given that the batch size and the hidden dimension don’t change. The greatest improvement occurs within a specific range (Region 2 in Figure 6); the speedup gradually decreases towards Region 1 or Region 3.

To understand this trend, we examined the runtime dependencies of each kernel on sequence length and number of heads:

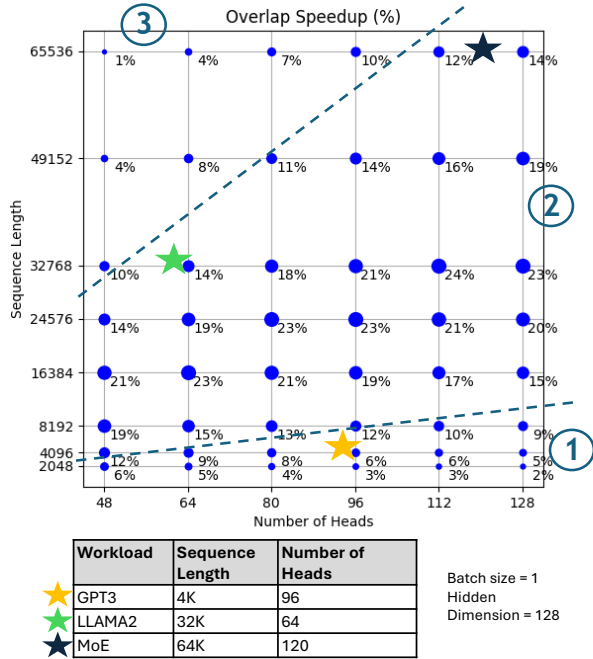


Figure 6. Overlap speedup across different sequence lengths and number of heads, using our theoretical performance model.

The GEMM layer’s runtime depends on the number of multiply-adds, which is  $M * N * K$ . For each of the four GEMM layers discussed in the paper, the M dimension is proportional to  $batch\_size(B) * sequence\_length(SQ)$ , and the N and K dimension is proportional to  $number\_of\_heads(nH) * hidden\_dimension(dH)$ :

$$Runtime(GEMM) = O(B * SQ * dH^2 * nH^2)$$

Similarly, the Attention runtime depends on the number of multiply-adds from the two matrix multiplication:

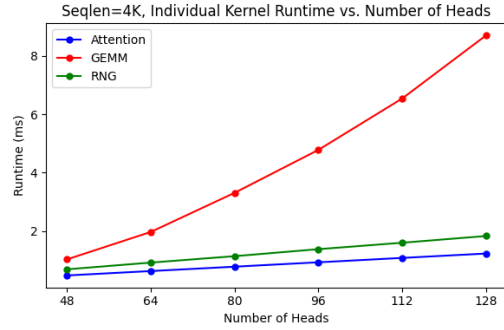
$$Runtime(Attention) = O(B * nH * dH * SQ^2)$$

The RNG runtime depends on the number of elements in the intermediate layer of Attention:

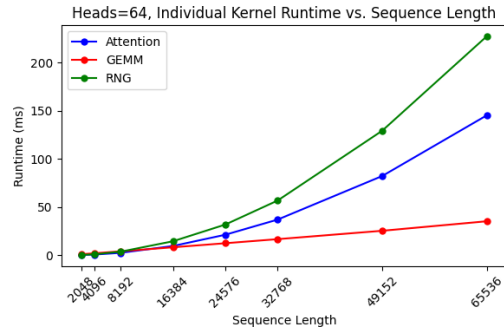
$$Runtime(RNG) = O(B * nH * SQ^2)$$

Figure 15 presents the runtime variation for each kernel across different sequence lengths and number of heads. The data shows that while GEMM runtime scales quadratically with the number of heads, the Attention and RNG runtime scales linearly. Conversely, Attention and RNG runtime scales quadratically with sequence length, whereas GEMM runtime scales linearly.

Analysis of the three regions highlighted in Figure 6 indicates:



(a) Individual kernel runtime with different number of heads.



(b) Individual kernel runtime with different sequence length.

Figure 7. Kernel runtime variation with different sequence length and number of heads, measured on silicon. GEMM runtime scales quadratically with number of heads, whereas Attention and RNG runtime scales quadratically with sequence length.

- Region 1 (low speedup): Overall runtime is dominated by GEMM layers due to a large number of heads and short sequence lengths. Overlapping offers limited benefits here.
- Region 2 (optimal speedup): Balances sequence length and number of heads, where RNG runtime is shorter but close to the GEMM runtime. Maximum benefits from hiding RNG latency by overlapping with GEMM.
- Region 3 (decreasing speedup): RNG runtime exceeds GEMM because of the long sequence lengths, leading to full exposure of RNG operations post-GEMM completion, diminishing the overlapping benefits.

Our analysis illustrates the conditional effectiveness of the overlapping strategy based on network parameters, offering insights for optimizing LLM training performance.

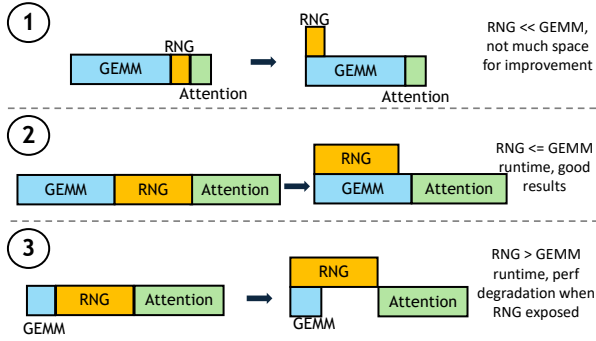


Figure 8. Analysis of speedup across three regions.

## 5 DISCUSSION

In this section, we dive into the stand-alone RNG’s HBM capacity requirement, and the overlapping methodology’s implication on different RNG implementations and future hardware architecture generations.

### 5.1 HBM Capacity Requirement for Stand-alone RNG

An overhead brought by our methodology is storing the RNG bits generated in HBM to be later used by the Attention kernel. For each element in Attention’s intermediate matrix, assuming RNG generates 1 bit per element to indicate the dropping status, we require storage of  $B * nH * SQ^2$  in HBM, which may initially appear to be critical.

Figure 9 illustrates the HBM requirements for stand-alone RNG when the entire network is run on a single GPU. If we hypothetically allocate 8GB for RNG data, it becomes apparent that applying this methodology to networks with sequence lengths of 32K or more is not feasible on a single GPU.

However, the typical deployment scenario for LLM training involves multiple GPUs, where the workload is divided into smaller segments distributed across the GPUs. This division significantly reduces the HBM capacity needed for RNG on each GPU. Common strategies for parallelism include Tensor Parallelism (Shoeybi et al., 2019) and Sequence Parallelism (Korthikanti et al., 2023), which split the head and sequence length dimensions, respectively. Figure 9 also demonstrates the reduced HBM requirements when employing these parallelism mechanisms. For the three mainstream LLM training networks, GPT3, LLAMA2 and GPT4-MoE, the required HBM capacity is decreased by a factor of ten or more, depending on the chosen parallelism strategy and dimension.

It is worth noting that parallelism does not change the performance benefit from overlapping RNG and GEMM analyzed

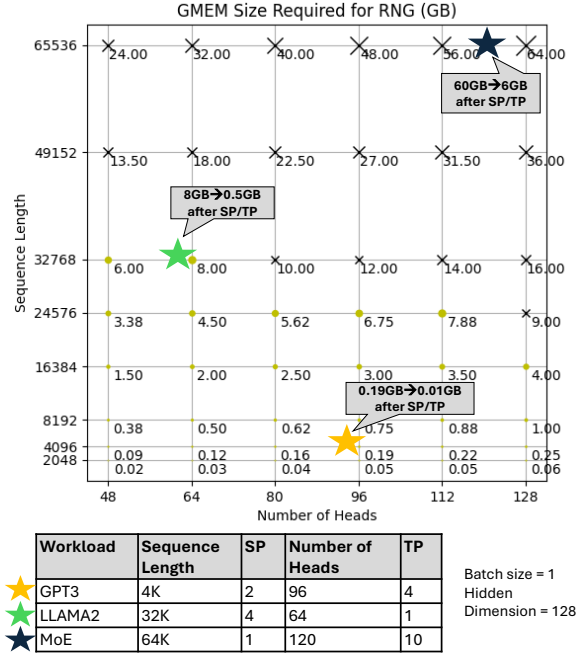


Figure 9. HBM capacity requirements for stand-alone RNG across different network configurations.

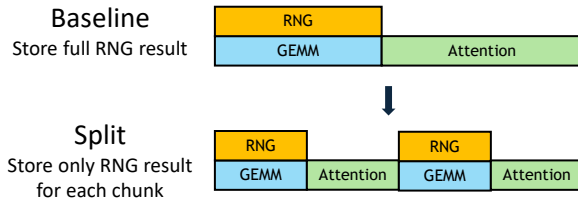


Figure 10. Pipelining kernels to further reduce HBM storage requirements.

earlier. Since the workload is split evenly on each GPU, the ratios of RNG, GEMM and Attention kernel runtime stay the same.

If parallelism across multiple GPUs is still not enough to alleviate HBM storage concerns, an additional strategy can be applied which involves pipelining the RNG, GEMM, and Attention kernels. Figure 10 illustrates this strategy. It involves processing only a portion of the total computation per kernel at a time, splitting along the sequence length dimension to avoid creating dependencies in the GEMM kernel.

Moreover, as depicted previously in Figure 2, implementing parallelism introduces communication layers within each Transformer Block. Fortunately, the runtime impact of these communication layers can also be minimized using the same pipelining technique. Since communication layers utilize

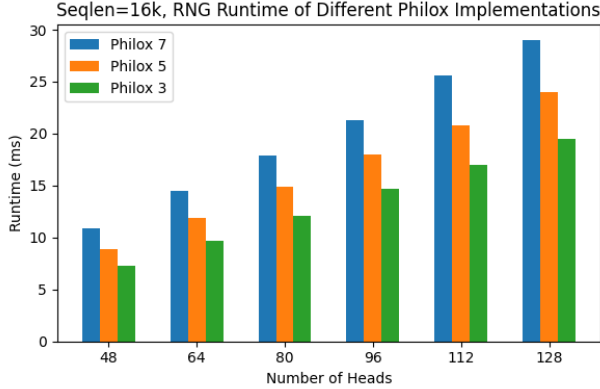


Figure 11. Silicon measurements of stand-alone RNG kernel runtime with different Philox implementations for a sequence length of 16K.

distinctly separate resources from GEMM (such as NVLink bandwidth), their concurrent execution will not introduce resource contention and will effectively hide communication latency.

## 5.2 Implication of Cheaper RNG

In our prior discussions, we focused on the use of Philox 7 for RNG implementation. This subsection explores the implications of adopting more cost-effective RNG implementations, namely Philox 5 and Philox 3, which involve fewer computational iterations and shorter runtimes.

We implemented all three Philox variants (Philox 3, 5, 7) on silicon using the GH100 with the same experimental setup as previously discussed. We show representative results collected for sequence length = 16K in Figure 11, which has a consistent trend with other configurations not shown on the graph.

We observed that the runtime of the Philox 5 RNG kernel is approximately 81% of that required for Philox 7, while Philox 3 operates at 67% of the Philox 7 runtime. These numbers align closely with the expected reduction in Fused Multiply-Add (FMA) operations (71% for Philox 5 and 43% for Philox 3). The difference is because other operations in the RNG process do not scale linearly with the number of iterations.

Our theoretical performance model was validated against the silicon results on overlapping RNG with QKV\_GEMM, showing an error margin consistent with previous validations. Using the validated model, we further analyzed the implications of varying RNG complexities on overlapping RNG with all four GEMM kernels in the Transformer Block.

As the complexity of the RNG algorithm decreases, the potential for speedup through overlapping also diminishes

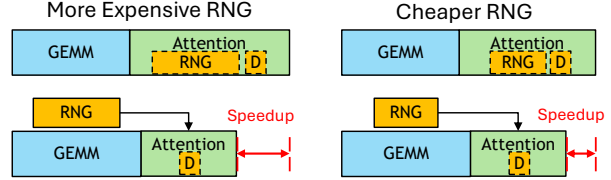


Figure 12. Cheaper RNG implementation results in smaller overall speedup.

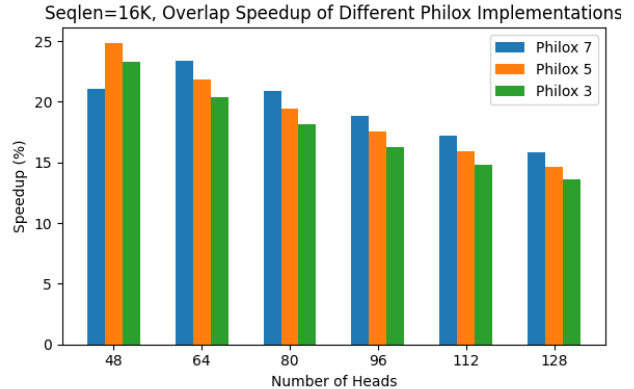


Figure 13. Overlap speedup with different RNG Philox implementations, derived from theoretical model.

because the runtimes of the Attention and GEMM kernels remain unchanged. Thus, cheaper RNG implementations should result in smaller overall savings, as shown in Figure 12. This is the case in most scenarios, as shown in Figure 13. However, in certain cases (such as Philox 7 implementation with number of heads = 48 and sequence length = 16K) the RNG runtime exceeds the GEMM runtime, introducing performance loss from fully exposed RNG after GEMM completes. This typically occurs with a smaller number of heads and a relatively long sequence length - Region 3 as discussed in Figure 6.

Moreover, we observed that the differences in speedup among various RNG implementations are relatively small. The standalone RNG kernel is primarily limited by the ALU pipeline, and the runtime decreases almost proportionally with the reduction in computation required. When RNG is fused into the Attention kernel, ALU is no longer the main bottleneck, and the performance depends on the Issue Stage where there is less difference between different RNG implementations. Consequently, the runtime reduction of the fused kernel is smaller than that of the standalone RNG kernel. Since the runtime of the GEMM kernel remains constant and the fused Attention-RNG kernel sees minimal changes, the overall speedup differences between the RNG implementations are relatively small.



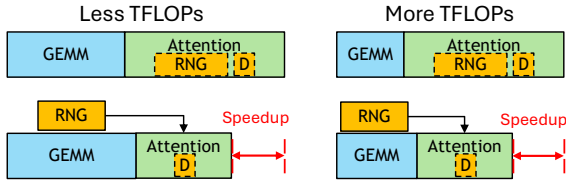


Figure 14. Overlap speedup with different GPU compute capability (TFLOPs). While GEMM runtime decreases, RNG and Attention runtimes remain constant, leading to a greater proportional speedup.

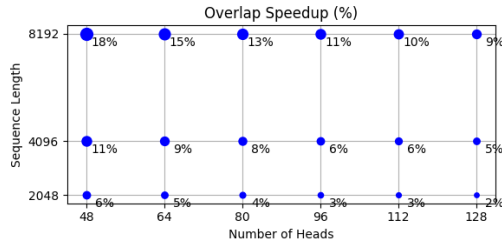
### 5.3 Hardware Exploration

Our analysis so far has been in the context of NVIDIA’s GH100 GPUs (NVIDIA, f). With our fine-grained performance model, we now explore how variations in hardware design might influence the efficiency of our overlapping strategy.

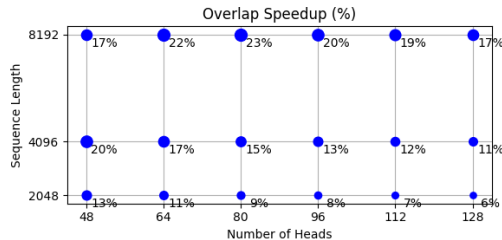
A key aspect of hardware evolution, particularly with NVIDIA GPUs, is the consistent increase of computational efficiency with each new generation. This trend continues with the newest Blackwell GPUs (NVIDIA, a), which motivates us to model the potential impacts of further advancements in computation power, such as enhanced FP operations or lower FP precisions.

Figure 15b illustrates the implications of increased compute capability on our overlapping technique. We maintain the assumption that computation remains the bottleneck for GEMM, with memory performance keeping pace with MMA improvements through reduced precision or increased memory bandwidth. However, other non-Tensor related limiters like the issue pipeline and the ALU pipeline are likely to remain unchanged, meaning the most significant runtime reduction would be observed in the GEMM kernel. This shift will make RNG latency an even more critical bottleneck, proportionally increasing its impact on end-to-end network performance. Although the absolute runtime difference between baseline and overlapped configurations remains similar, the relative speedup should improve.

We evaluated the theoretical performance of our overlapping strategy using a hypothetical model of a more advanced GPU, which offers twice the compute capability of the H100. Figure 15 shows that overall speedup increases up to 10% with higher compute efficiency for a variation of sequence lengths and number of heads. Our findings indicate that while reductions in GEMM runtime boost the overall speedup ratio, this benefit is primarily observed in workloads with shorter sequence lengths. For longer sequences, where RNG and Attention dominate network runtime, overlapping a shorter GEMM could exacerbate problems by fully exposing RNG latency once GEMM computation com-



(a) Overlap speedup on GH100.



(b) Overlap speedup on a hypothetical GPU where the GEMM compute capability is doubled and non-Tensor limiters remain the same.

Figure 15. Overlap speedup increases with more GEMM compute capability on relatively short sequence lengths and varying number of heads.

pletes. Thus, it is more advantageous to overlapping RNG and GEMM computation for hardware with high computational efficiency and workloads featuring relatively shorter (8K or smaller) sequence lengths.

This analysis underscores the need for next-generation hardware to consider optimizing traditionally non-Tensor related factors. On the other hand, if hardware optimization on these factors are not possible, we call for future hardware-software co-design to value kernel overlapping: efficient libraries can be developed to facilitate the overlapping of non-GEMM operations, which typically do not consume extensive computation and memory resources, with GEMM operations.

## 6 RELATED WORK

Scheduling layer components within Large Language Models (LLMs) has become a critical area of research due to the increasing demands of improving the efficiency of these models (Ye et al., 2024) (Li et al., 2024). Effective scheduling can improve end-to-end network performance when components underutilize GPU resources, if they exhibit distinct resource utilization patterns.

Several studies have explored different aspects of LLM scheduling. For instance, Splitwise (Patel et al., 2024) proposes a technique to separate the prefill and decoding phases of LLM inference onto different machines because of their

unique characteristics. Similarly, Muxserve (Duan et al.) introduces a spatial-temporal multiplexing system that can flexibly colocate or separate these phases to maximize run-time efficiency.

A popular scheduling approach involves overlapping computation-intensive components, such as matrix multiplications (matmuls) that utilize floating-point (FP) units, with inter-GPU communication tasks. The large sizes of LLM networks often require the workload to be divided executed in parallel on multiple GPUs, where communication layers are required. Several forms of parallelism have been proposed to enhance efficient model training and serving, including Data Parallelism (Li et al., 2020), Tensor Parallelism (Shoeybi et al., 2019), Expert Parallelism (Rajbhandari et al., 2022)(NVIDIA, g), and Sequence Parallelism (Li et al., 2021). Since there is dependency between data on different GPUs, parallelism involve essential communication layers that transfer large amount of data between each GPU. Given the substantial communication overhead and distinct resource requirements between the data-transfer-heavy communication layers and the computation-heavy GEMM layers, it is ideal to overlap them to improve run-time. Best practices suggest splitting these components into finer-grained chunks and pipelining them for efficient overlapping (Pati et al., 2024)(NVIDIA, b). This method is often enhanced by fine-grained kernel fusion techniques to further optimize performance (Chang et al., 2024)(Punniyamurthy et al., 2023).

In addition, several theoretical frameworks have been developed to model and analyze LLM workload performance by pinpointing hardware bottlenecks. Examples include roofline models (Yuan et al., 2024), large-scale simulation framework (Agrawal et al., 2024b)(Agrawal et al., 2024a), and light-weight performance modeling approaches (Zhang et al., 2024). Our work uses a similar approach of analyzing LLM training performance based on hardware constraints, and extends these methodologies by providing detailed insights into the effectiveness of layer overlapping strategies.

## 7 CONCLUSION

This paper proposed a strategic overlapping of RNG with GEMM layers to improve end-to-end LLM training efficiency. By decoupling RNG from the Dropout process and running it in parallel with the computationally intense GEMM operations, we effectively reduce the latency impact typically associated with RNG if fused with the Attention layer. Our approach optimizes the use of hardware resources by exploiting the distinct hardware demands of RNG and GEMM, and achieves a notable improvement in end-to-end training performance, with speedups ranging from 1.06x to 1.23x within a Transformer Block across various LLM architectures.

We also develop a fine-grained theoretical performance model, validated with silicon results, to provide deeper insights into overlapping different kernels in the LLM network and highlight potential areas for further improvements. The principles established here can extend to optimizing other network layers, offering a generalized strategy to analyze the implications and enhance the performance of future LLM systems. As LLMs continue to scale and the demand for computational efficiency grows, the theoretical model can serve as a valuable framework for evaluating future overlapping strategies maximize resource utilization and minimize training time.

## REFERENCES

- Agrawal, A., Agarwal, A., Kedia, N., Mohan, J., Kundu, S., Kwatra, N., Ramjee, R., and Tumanov, A. Metron: Holistic performance evaluation framework for llm inference systems. *arXiv preprint arXiv:2407.07000*, 2024a.
- Agrawal, A., Kedia, N., Mohan, J., Panwar, A., Kwatra, N., Gulavani, B., Ramjee, R., and Tumanov, A. Vidur: A large-scale simulation framework for llm inference. *Proceedings of Machine Learning and Systems*, 6:351–366, 2024b.
- Brown, T. B. Language models are few-shot learners. *arXiv preprint arXiv:2005.14165*, 2020.
- Chang, L., Bao, W., Hou, Q., Jiang, C., Zheng, N., Zhong, Y., Zhang, X., Song, Z., Jiang, Z., Lin, H., et al. Flux: Fast software-based communication overlap on gpus through kernel fusion. *arXiv preprint arXiv:2406.06858*, 2024.
- Dao, T. Flashattention-2: Faster attention with better parallelism and work partitioning. *arXiv preprint arXiv:2307.08691*, 2023.
- Dao, T., Fu, D., Ermon, S., Rudra, A., and Ré, C. Flashattention: Fast and memory-efficient exact attention with io-awareness. *Advances in Neural Information Processing Systems*, 35:16344–16359, 2022.
- Duan, J., Lu, R., Duanmu, H., Li, X., Zhang, X., Lin, D., Stoica, I., and Zhang, H. Muxserve: Flexible spatial-temporal multiplexing for multiple llm serving. In *Forty-first International Conference on Machine Learning*.
- Face, H. Transformers - llama [github]. URL [https://github.com/huggingface/transformers/blob/main/src/transformers/models/llama/modeling\\_llama.py#L470](https://github.com/huggingface/transformers/blob/main/src/transformers/models/llama/modeling_llama.py#L470).
- II, S. M. W. Everything we know about gpt-4, 2023. URL <https://klu.ai/blog/gpt-4-llm>.

- Kerr, A., Merrill, D., Demouth, J., and Tran, J. Cutlass: Fast linear algebra in cuda c++. URL <https://developer.nvidia.com/blog/cutlass-linear-algebra-cuda/>.
- Korthikanti, V. A., Casper, J., Lym, S., McAfee, L., Andersch, M., Shoeybi, M., and Catanzaro, B. Reducing activation recomputation in large transformer models. *Proceedings of Machine Learning and Systems*, 5:341–353, 2023.
- Li, B., Jiang, Y., Gadepally, V., and Tiwari, D. Llm inference serving: Survey of recent advances and opportunities. *arXiv preprint arXiv:2407.12391*, 2024.
- Li, C., Li, J., Kaatz, A., Krashinsky, R. M., and Xu, A. Thread specialization for collaborative data transfer and computation, May 11 2023. US Patent App. 17/689,660.
- Li, S., Zhao, Y., Varma, R., Salpekar, O., Noordhuis, P., Li, T., Paszke, A., Smith, J., Vaughan, B., Damania, P., et al. Pytorch distributed: Experiences on accelerating data parallel training. *arXiv preprint arXiv:2006.15704*, 2020.
- Li, S., Xue, F., Baranwal, C., Li, Y., and You, Y. Sequence parallelism: Long sequence training from system perspective. *arXiv preprint arXiv:2105.13120*, 2021.
- Liu, Z., Xu, Z., Jin, J., Shen, Z., and Darrell, T. Dropout reduces underfitting. In *International Conference on Machine Learning*, pp. 22233–22248. PMLR, 2023.
- NumPy. Philox counter-based rng. URL [https://numpy.org/doc/stable/reference/random/bit\\_generators/philox.html](https://numpy.org/doc/stable/reference/random/bit_generators/philox.html).
- NVIDIA. Nvidia blackwell architecture technical brief, a. URL <https://resources.nvidia.com/en-us-blackwell-architecture>.
- NVIDIA. Communication overlap, b. URL [https://docs.nvidia.com/nemo-framework/user-guide/latest/nemotoolkit/features/optimizations/communication\\_overlap.html](https://docs.nvidia.com/nemo-framework/user-guide/latest/nemotoolkit/features/optimizations/communication_overlap.html).
- NVIDIA. Getting started with cuda graphs, c. URL <https://developer.nvidia.com/blog/cuda-graphs/>.
- NVIDIA. Curand, d. URL <https://docs.nvidia.com/cuda/curand/device-api-overview.html>.
- NVIDIA. Fp8 for deep learning, e. URL <https://www.nvidia.com/en-us/on-demand/session/gtcspring23-s52166/>.
- NVIDIA. Nvidia h100 tensor core gpu architecture, f. URL <https://www.nvidia.com/en-us/data-center/h100/>.
- NVIDIA. Scaling language model training to a trillion parameters using megatron, g. URL <https://developer.nvidia.com/blog/scaling-language-model-training-to-a-trillion-par>.
- NVIDIA. Demystifying ai inference deployments for trillion parameter large language models, h. URL <https://developer.nvidia.com/blog/demystifying-ai-inference-deployments-for-trillio>.
- NVIDIA. Spatial partitioning (also known as warp specialization), i. URL <https://docs.nvidia.com/cuda/cuda-c-programming-guide/index.html#spatial-partitioning-also-known-as-warp-specializ>.
- OpenAI. Gpt-4 technical report, 2023.
- Patel, P., Choukse, E., Zhang, C., Shah, A., Goiri, Í., Maleki, S., and Bianchini, R. Splitwise: Efficient generative llm inference using phase splitting. In *2024 ACM/IEEE 51st Annual International Symposium on Computer Architecture (ISCA)*, pp. 118–132. IEEE, 2024.
- Pati, S., Aga, S., Islam, M., Jayasena, N., and Sinclair, M. D. T3: Transparent tracking & triggering for fine-grained overlap of compute & collectives. In *Proceedings of the 29th ACM International Conference on Architectural Support for Programming Languages and Operating Systems, Volume 2*, pp. 1146–1164, 2024.
- Punniyamurthy, K., Hamidouche, K., and Beckmann, B. M. Optimizing distributed ml communication with fused computation-collective operations. *arXiv preprint arXiv:2305.06942*, 2023.
- Rajbhandari, S., Li, C., Yao, Z., Zhang, M., Aminabadi, R. Y., Awan, A. A., Rasley, J., and He, Y. Deepspeed-moe: Advancing mixture-of-experts inference and training to power next-generation ai scale. In *International conference on machine learning*, pp. 18332–18346. PMLR, 2022.
- Salmon, J. K., Moraes, M. A., Dror, R. O., and Shaw, D. E. Parallel random numbers: as easy as 1, 2, 3. In *Proceedings of 2011 international conference for high performance computing, networking, storage and analysis*, pp. 1–12, 2011.
- Schumacher, D. Attention dropout. URL <https://serp.ai/attention-dropout/>.

- Shah, J., Bikshandi, G., Zhang, Y., Thakkar, V., Ramani, P., and Dao, T. Flashattention-3: Fast and accurate attention with asynchrony and low-precision. *arXiv preprint arXiv:2407.08608*, 2024.
- Shastri, Y. Attention mechanism in llms: An intuitive explanation. URL <https://www.datacamp.com/blog/attention-mechanism-in-llms-intuition>.
- Shoeybi, M., Patwary, M., Puri, R., LeGresley, P., Casper, J., and Catanzaro, B. Megatron-lm: Training multi-billion parameter language models using model parallelism. *arXiv preprint arXiv:1909.08053*, 2019.
- Srivastava, N., Hinton, G., Krizhevsky, A., Sutskever, I., and Salakhutdinov, R. Dropout: a simple way to prevent neural networks from overfitting. *The journal of machine learning research*, 15(1):1929–1958, 2014.
- TensorFlow. Random number generation. URL [https://www.tensorflow.org/guide/random\\_numbers#general](https://www.tensorflow.org/guide/random_numbers#general).
- Touvron, H., Martin, L., Stone, K., Albert, P., Almahairi, A., Babaei, Y., Bashlykov, N., Batra, S., Bhargava, P., Bhosale, S., et al. Llama 2: Open foundation and fine-tuned chat models. *arXiv preprint arXiv:2307.09288*, 2023.
- Wan, L., Zeiler, M., Zhang, S., Le Cun, Y., and Fergus, R. Regularization of neural networks using dropconnect. In *International conference on machine learning*, pp. 1058–1066. PMLR, 2013.
- Xue, F., Fu, Y., Zhou, W., Zheng, Z., and You, Y. To repeat or not to repeat: Insights from scaling llm under token-crisis. *Advances in Neural Information Processing Systems*, 36, 2024.
- Ye, Z., Gao, W., Hu, Q., Sun, P., Wang, X., Luo, Y., Zhang, T., and Wen, Y. Deep learning workload scheduling in gpu datacenters: A survey. *ACM Computing Surveys*, 56(6):1–38, 2024.
- Yuan, Z., Shang, Y., Zhou, Y., Dong, Z., Xue, C., Wu, B., Li, Z., Gu, Q., Lee, Y. J., Yan, Y., et al. Llm inference unveiled: Survey and roofline model insights. *arXiv preprint arXiv:2402.16363*, 2024.
- Zehui, L., Liu, P., Huang, L., Chen, J., Qiu, X., and Huang, X. Dropattention: A regularization method for fully-connected self-attention networks. *arXiv preprint arXiv:1907.11065*, 2019.
- Zhang, H., Ning, A., Prabhakar, R. B., and Wentzlaff, D. Llmcompass: Enabling efficient hardware design for large language model inference. In *2024 ACM/IEEE*

*51st Annual International Symposium on Computer Architecture (ISCA)*, pp. 1080–1096. IEEE, 2024.